

Fumagillin Prodrug Nanotherapy Suppresses Macrophage Inflammatory Response *via* Endothelial Nitric Oxide

Hui-fang Zhou^{1‡}, Huimin Yan^{1‡}, Ying Hu¹, Luke E. Springer¹, Xiaoxia Yang², Samuel A.
Wickline², Dipanjan Pan^{2†}, Gregory M. Lanza^{2*}, Christine T.N. Pham^{1*}

¹Division of Rheumatology and ²Division of Cardiology, Department of Medicine, Washington
University School of Medicine, Saint Louis, MO USA

‡These authors contributed equally

Corresponding Authors

* Christine Pham, Division of Rheumatology, Department of Medicine, Washington
University School of Medicine, 660 South Euclid Avenue, Box 8045, Saint Louis, MO 63110
USA. Phone: 314-362-9043. Fax: 314-454-1091. Email: cpham@dom.wustl.edu

* Gregory Lanza, Division of Cardiology, Department of Medicine, Washington University
School of Medicine, 660 South Euclid Avenue, Box 8215, Saint Louis, MO 63110 USA. Phone:
314-454-8813 Fax: 314-454-5265. Email: greg.lanza@mac.com

Present Addresses

† Bioengineering and Beckman Institute, University of Illinois at Urbana-Champaign, Urbana,
IL USA

Supplementary Information

Methods

Quantitative analysis of immunofluorescence

Mouse paws were harvested on day 9 after serum transfer, embedded in OCT compound and sectioned at 9 μ m. Sections were fixed in 4% paraformaldehyde, blocked in 8% BSA in PBS, and incubated with a PE-conjugated anti-mouse F4/80 antibody (1:100 dilution, Cat. 12-4801, eBioscience) and FITC-conjugated anti-mouse CD206 antibody (1:400 dilution, Cat. 141704 Biolegend) or anti-mouse phospho-p65 (1:100 dilution, Cat. 3033, Cell Signaling), followed by FITC-conjugated donkey anti-rabbit antibody (1:100 dilution; Jackson ImmunoResearch).

All fluorescent images were visualized on a Nikon Eclipse fluorescence microscope and acquired with QCapture software using the same time exposure. Merged and single-color images were loaded into ImageJ software (<http://rsb.info.nih.gov/ij>) for analysis. Threshold color of all images was set to the same hue, saturation, and brightness. Using the brightness to mark the picture, single (phospho-p65⁺) and double (F4/80⁺CD206⁺) positively stained areas were selected and the ROIs were measured on the unfiltered images. For fluorescence quantification, single-color pictures were loaded into ImageJ software and positive areas selected for analysis. The data were presented as integrated OD (IntDen) and normalized to the control group. Data were obtained from six to eight fields per section and four to five paw sections per treatment group.

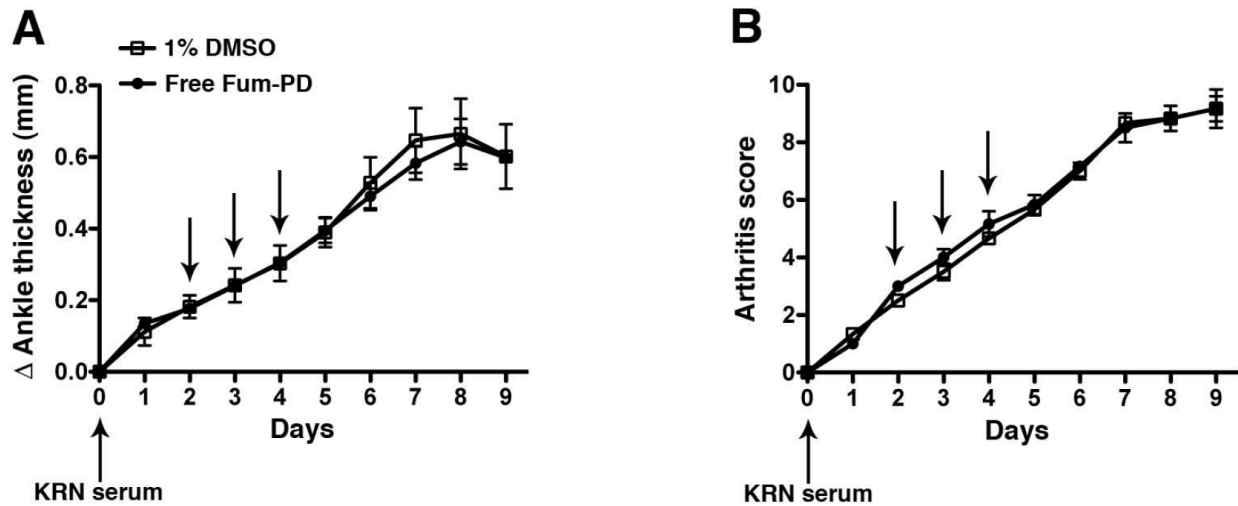


Fig. S1. Free Fum-PD is ineffective at suppressing KRN arthritis. Mice were injected i.p. with 150 μ l of KRN serum on day 0. Changes in ankle thickness (**A**) and arthritis score (**B**) were assessed daily. Starting on day 2, when early arthritis was clearly established, mice were randomly divided into 2 groups and given serial daily injections (x3, arrows) of free Fum-PD at 0.3 μ g/g body weight in 1% DMSO/PBS or 1% DMSO in PBS as control. Values represent mean \pm SEM of 3 mice per treatment condition. No difference in clinical indices was noted between treatment groups.

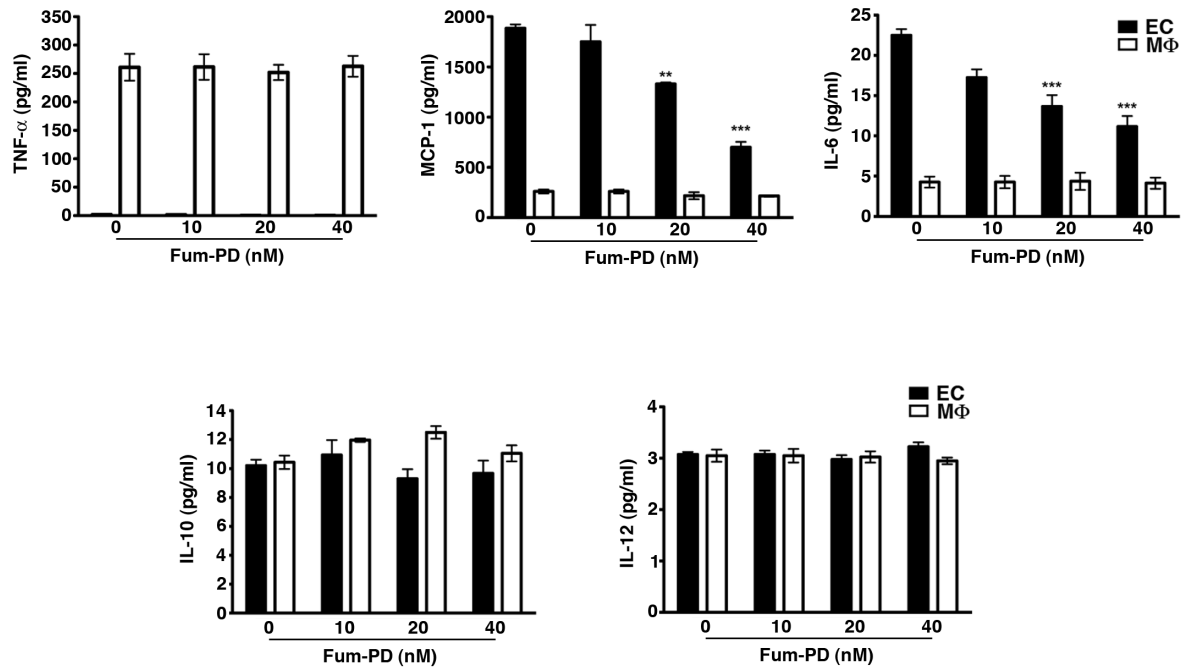


Fig. S2. Cytokine response *in vitro* following Fum-PD exposure. SEVC4 endothelial cells (EC) and day-5 thioglycollate elicited macrophages (M Φ) were cultured with indicated Fum-PD concentrations or 0.1% DMS0 (0 nM Fum-PD). At 48 h the supernatants were harvested and assayed for cytokine levels by cytometric bead array (CBA). Values represent mean \pm SEM of triplicate samples derived from 5 independent experiments. **P < 0.01, ***P < 0.001. NB, Fum-PD has no direct effect on TNF- α , MCP-1, and IL-6 release by M Φ . On the other hand, increasing concentrations of Fum-PD led to dose-dependent decrease in MCP-1 and IL-6 release by EC, likely secondary to EC apoptosis (Fig. 3C)

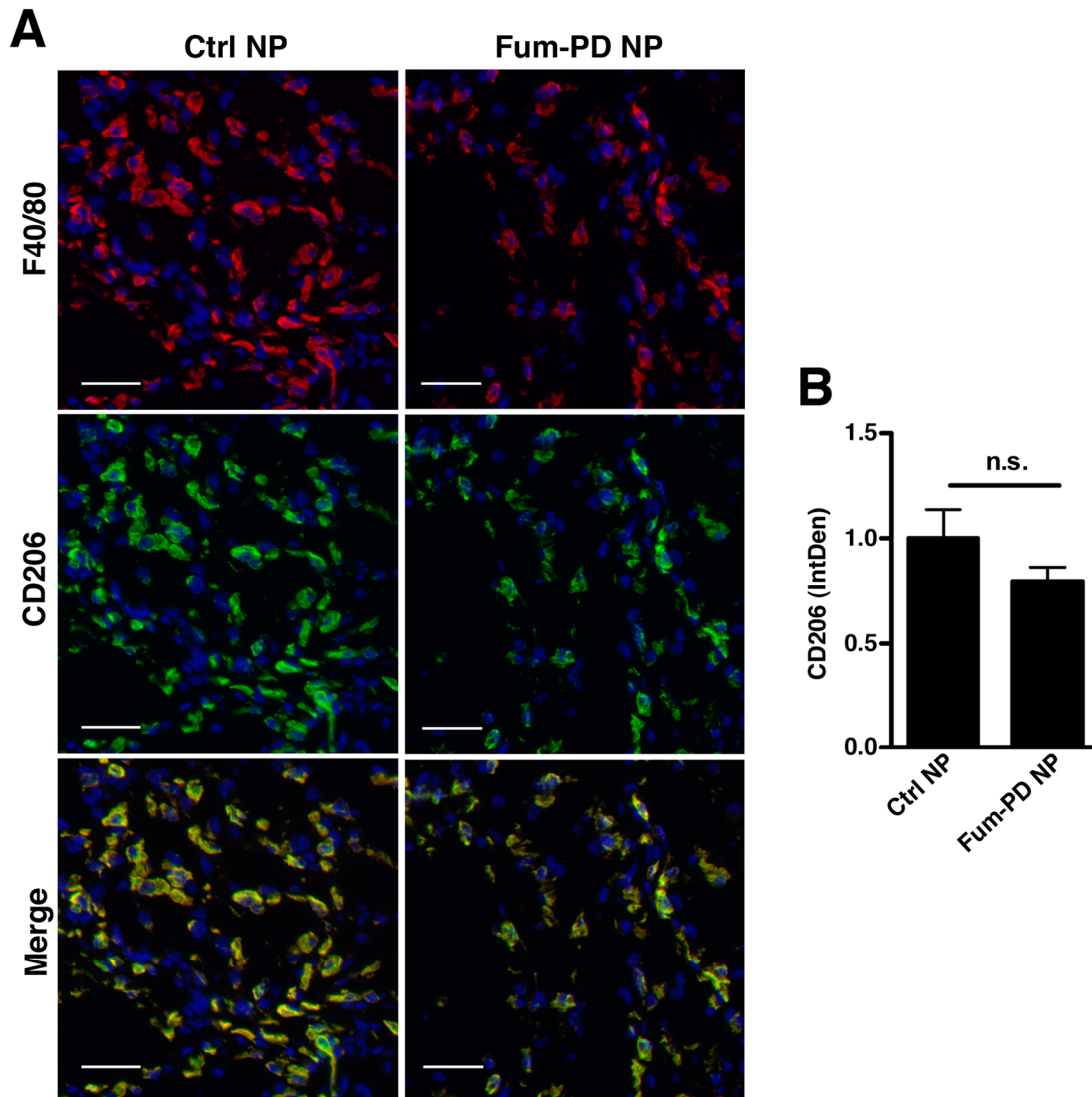


Fig. S3. Alternatively activated M2 macrophages predominate in chronic phase of arthritis. (A) Day 9 paw sections from mice treated with Ctrl NP or Fum-PD NP were stained for macrophages with F4/80 (red) and mannose receptor CD206 (green) expressed on alternatively activated macrophages (M2). Co-localization of F4/80 and CD206 appears yellow in merged figures. Note that alternatively activated macrophages predominate in day 9 synovium, regardless of treatment. (B) CD206 immunofluorescence level (IntDen) was calculated using ImageJ program as detailed in the Supplementary Methods section above. Values represent mean \pm SEM of 4 paws per condition. Scale bar = 50 μ m. n.s., not significant.

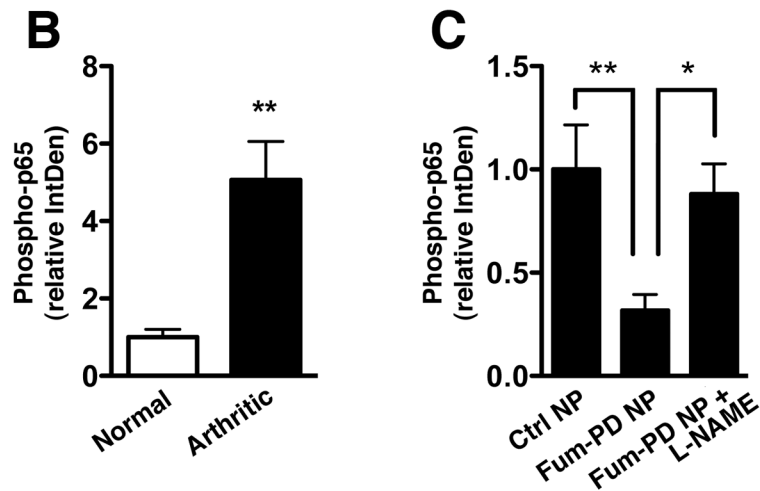
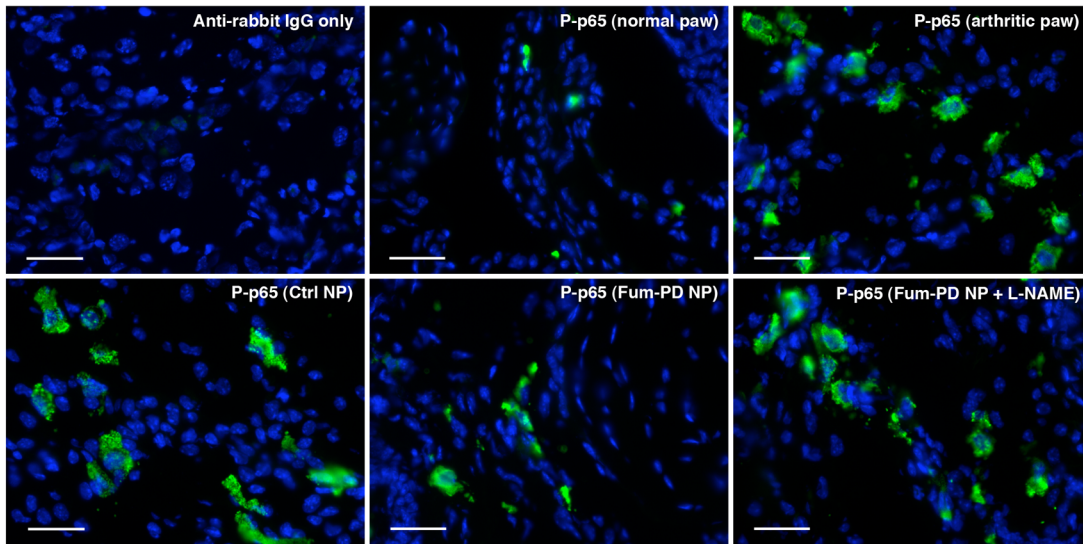
A

Fig. S4. Fumagillin nanotherapy-mediated NF- κ B p65 suppression is NO-dependent. (A) Normal or day 9 arthritic paws were stained with an antibody specific for phospho (P)-p65 (green). Scale bar = 50 μ m. (B) The relative immunofluorescence level (IntDen) of phospho-p65 in normal and day 9 arthritic paws were calculated using ImageJ program as detailed in the Supplementary Methods section above. (C) Relative immunofluorescence level (IntDen) of phospho-p65 is expressed relative to the level obtained for Ctrl NP, which was set at 1. Values represent mean \pm SEM of 4 paws per condition. *P < 0.05, **P < 0.01.

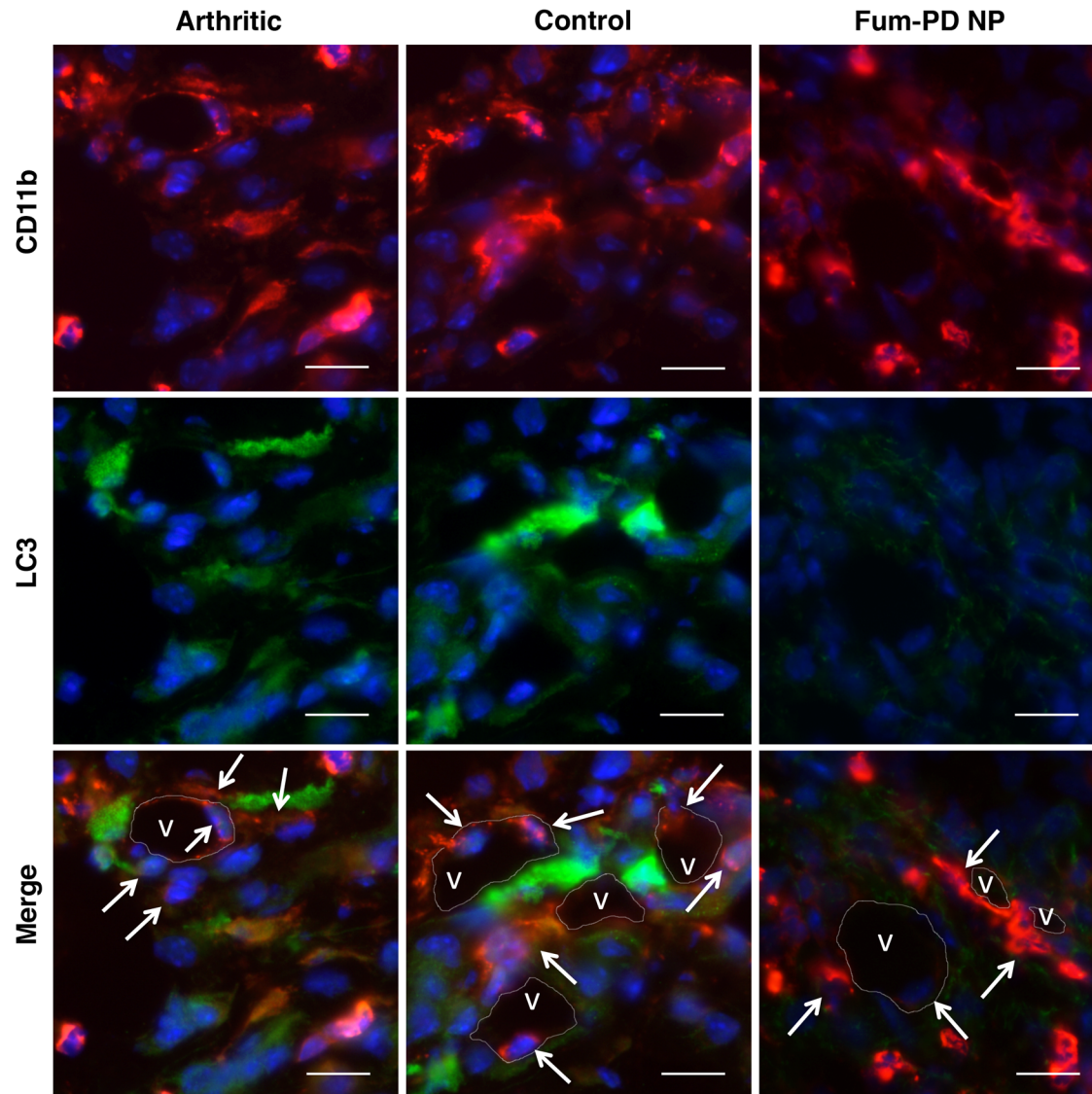


Fig. S5. Endothelial-macrophage tight interactions in the inflamed synovium. Day 9 sections of arthritic paws obtained from different treatment groups were stained for CD11b (red, indicating mainly macrophages and granulocytes) and LC3 (green). DAPI stained nuclei blue. Note the tight association between CD11b⁺ cells (arrows) and the endothelium. It is likely that this tight endothelial-macrophage interaction provides the critical signals (such as NO) that lead to autophagy modulation, macrophage activation and/or polarization. However, we cannot rule out indirect effects on macrophages through secreted mediators from the synovial milieu (i.e. cytokines). Note the relative low level of LC3 in CD11b⁺ cells in the Fum-PD treated animals. Scale bar = 20 μ m.